International Journal of Civil Engineering and Technology (IJCIET)
Volume 9, Issue 9, September 2018, pp. 1791–1800, Article ID: IJCIET_09_09_173
Available online at http://www.iaeme.com/ijciet/issues.asp?JType=IJCIET&VType=9&IType=9
ISSN Print: 0976-6308 and ISSN Online: 0976-6316

CONTROLLED MORPHOLOGY OF SILVER NANOPARTICLES BY ETCHING LASER WAVELENGTH

Wail H. Ali
Mechatronic Engineering Department, Technical Engineering College,
Middle Technical University, Baghdad, Iraq

ABSTRACT

In this study, the influences of etching laser wavelength on the surface morphology of silver nanoparticles AgNPs deposited on macro porous silicon (mPSi) substrates were studied. Laser assisted etching (LAE) process with different laser etching wavelengths 405nm, 635nm and 810nm were used to prepared different pores shape of pore-like structures macro- porous silicon layer. AgNPs was prepared by immersion plating with fixed deposition conditions. Structural and morphological characterizations of (mPSi) and AgNPs were inspected through studying of scanning electron microscope (SEM) and X-ray Diffraction (XRD) pattern of (mPSi) and AgNPs. These measurements indicated that the morphology of AgNPs were in different shape, sizes and distribution. This modification is strongly influenced by the etching laser wavelength used in the etching process. It was found that the AgNPs planes, grain size, specific surface area, and nucleation sites of silver nanoparticles toughly depended on chemical species and morphology mPSi.

Keywords: Porous silicon; laser assisted etching; silver nanoparticles.

Cite this Article: Wail H. Ali, Controlled Morphology of Silver Nanoparticles by Etching Laser Wavelength, International Journal of Civil Engineering and Technology, 9(9), 2018, pp. 1791–1800.

http://www.iaeme.com/IJCIET/issues.asp?JType=IJCIET&VType=9&IType=9

1. INTRODUCTION

mPSi has numerous exclusive morphologies properties including very large specific area, different pores form and sizes [1]. The chemical surfaces of porous matrix porous make it a very helpful material for catalytic applications [2]. Laser –assisted etching process of silicon in hydro fluoride (HF) acid having electrolytes intimations to pore creation for a low values of laser power density and to electro polishing for high applied laser power density. The controlling of laser parameters (power density and wavelength) is supplemented by variation of the porous surface morphology of etched surface. The etching rate at the interface between

the silicon and HF acid is governed by the laser parameters. Most of applications depend on the surface morphology of porous silicon [3,4].

The Si -H terminated dangling bonds and its position on the surface of mPSi represent as an efficient way of reducing silver ions without addition any reducing agent [6]. The unique physical and chemical of Silver nanoparticles deposition within the porous matrix substrate is of specific significance due to its chemical and biological uses. The typical features of AgNPs have been employed in extensive variety of potential applications like the detection process of gas vapors and chemical dissolved materials, medicine and renewable energies [7]. The influence of pore sizes and shape in the n-type meso porous structure on the morphological properties of the AgNPs was investigated extensively [8,9], and they recognized the ability of porous surface to reduce silver ions leads to the creation of Silver nanoparticles located on surface, with nearly no diffusion of the silver into the pores. In this work, we studied the influences of laser wavelength on the formation and preparation mechanism of AgNPs via silver ion reduction process. The morphological properties of the deposited AgNPs were studied by analyzing the SEM, FTIR, and XRD results.

2. EXPERIMENTAL DETAILS

2.1. Preparation of PSi samples

Three types of mPSi of pores morphologies were synthesized by LAE process of n-type with resistivity 100 Ω.cm phosphor-doped silicon wafer (100) orientation by using three laser wavelengths 405nm (violet) , 635nm (red) laser diodes and 810nm (infrared) . The starting Si substrate was cut into 3×3cm samples, cleaned in peroxide ammonia solution, Silicon substrate were immersed for a 10 min. into 10% aqueous hydrofluoric acid to remove the native oxide layer.

The etching procedure was occurred in specially designed cell which consisted of two-electrode system silicon substrate as an anode and a platinum ring as cathode. The experiment was carried out in room temperature and is presented in figure. 1. The cell donated us a mPSi layer of identical cross sectional region. (well recommended) mPSi. Solution of 48% HF in ethanol in proportions HF:C_2H_5OH as (1:1) was used as etchant. Morphological properties of mPSi were modified by the variation laser wavelength.

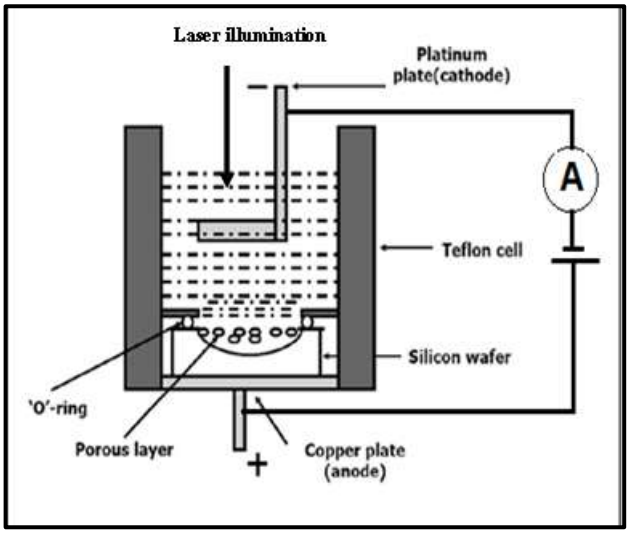

Figure 1 The schematic diagram of etching process.

The series of mPSi substrates were prepared at constant value of etching current density (J) of 35 mA/cm^2 and etching time (t) of 16 minutes throughout the substrate preparation. The etching procedure was taken on at fixed illumination intensity of 30 mW/cm^2. The mPSi substrates were cut into two parts. The first one was used for the assessment of morphological properties of mPSi, and the second part was used for formation AgNPs. The silver nanoparticles were prepared by immersion plating the mPSi sample in 10^{-2}M of $AgNO_3$ solution with fixed immersion time of about 10 minutes. The scanning electron microscopy (FE-SEM, GEMINR-SUPRA -35 VP- Carl Zeiss), X-ray diffraction (XRD-6000, Shemadzue) and Fourier transfer infrared (FTIR) spectrometer analyses were carried out by (PerKin –Elmer spectrometer).

3. RESULTS AND DISCUSSIONS

3.1. Preparation AgNPs on mPSi layer

Immersion plating process of porous silicon in AgNO3 solutions is an efficient process to create Ag nanoparticles through a redox process containing Ag+ ions with the hydrides situated on the porous surface. This process leads to a instantaneous creation of Ag nanoparticles through silver ions reduction by Si–H bonds concentrated within the porous matrix. Due to this process, nuclei of Ag crystals are formed at the pore boundaries and inside the pores itself, so the porous surface is progressively covered with a layer of silver regions [6]. Immersion plating process was carried out at fixed $AgNO_3$ concentration of about 10^{-3} M and fixed immersion time of about 10 min.

3.2. Properties of mPSi layer

The morphological features of mPSi layer comprise porosity, layer thickness and the pore sizes and shapes. The morphology plays a significant role in preparation of AgNPs since it's affords a great density of suitable locations for nucleation and creation of AgNPs. The morphological of mPSi layer are influenced by etching conditions: the current density, and the etching wavelength [10]. To vary the morphology especially the porosity, pores shape, and size, the etching laser wavelength has been changed. The porosity and the layer thickness of the porous layer is the restrictive factor which is known as the extent of void spaces within the layer. It is calculated via the gravimetric measurements [11]. The value of the porosity and the layer thicknesses as a function to etching laser wavelength is illustrated in table 1. The porosity of the fabricated porous layer at short laser wavelength is higher than that of the longer wavelength, while the layer thickness for porous samples is increased with increasing etching laser wavelength. this behavior may be owing to increase the density and size of the pores in the porous layer, due to the fact that the absorption process is inversely proportional with wavelength. The absorption depth and therefore the layer is defined as the inverse of an absorption coefficient at which the layer synthesized carriers e-h pairs are exponentially decreased by a factor of 1/2.7. The theoretical value of absorption depth is about 0.09µm, 3.7µm and 11 µm for laser wavelength 405 nm , 635nm and 810nm respectively [12].

Table 1 Porosity l and layer thickness of mPSi layer as a function to etching wavelength.

laser wavelengths	Porosity%	Porous layer thickness µm
405nm (violet)	82	1.2
635nm (red)	73	5.4
810nm (infrared)	61	12

Surface morphology of as prepared mPSi was studied through FE-SEM images of porous surface. The morphological characteristics of the porous layer like the pore width pore shape

and silicon spacing between adjacent pores were strongly dependent on the preparation conditions.

Figure, 2 demonstrations the top-view of surface topography of mPSi for three laser wavelengths. It was found that the resultant porous structure, as revealed in figure. 2, has a pore-like fine structure with different pores shapes and pore widths.

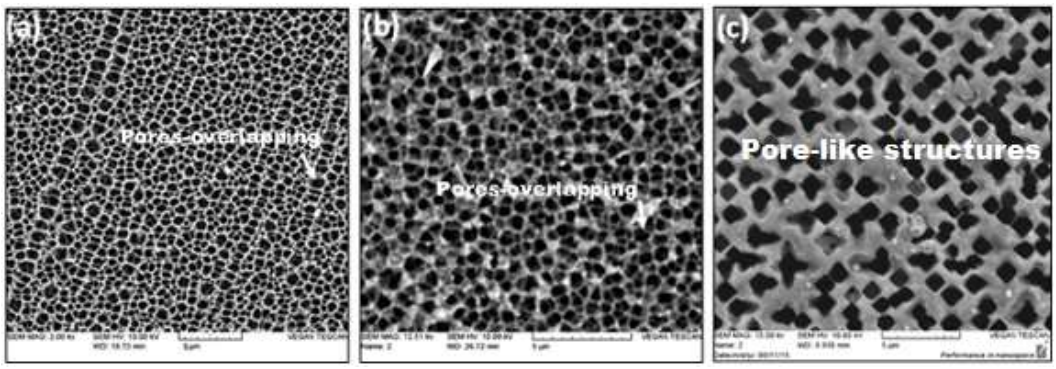

Figure 2 Display, the (FE-SEM) image of mPSi surface prepared by laser-assisted etching with illumination wavelengths (a) 405 nm, (b) 635 nm, and (c) 810 nm.

The top view of the surface reveals that the layer consists of a dense small pore aligned in irregular way. Array of void regions (dark) pores in Si matrix bright can be seen clearly in the top view FE-SEM images. The lessening of laser wavelength means an increase of silicon dissolution process within the upper porous layer due to the increase of photo-generated holes' number on the silicon electrode. This would allow favored dissolution between nearest-neighbour pores, there by promoting the pore-pore intersection. Though, etching rates may be different and this leads to non-uniformity in the values of the pores diameter. Different etching rates lead to non-uniformity in value of pores width arises from non-uniform laser power density distribution of illumination. This leads to non-uniform photo-generation holes, subsequent in different pore width. The non-uniform laser intensity of illumination may be attributed to the gradual decrease of laser intensity from its peak to the minimum value (Gaussian–beam distribution). The statistical distribution of the pore dimensions in the mPSi structure is shown in the figure.3. From this figure the average porous dimensions ranging from 0.06µm to 0.97µm while the peak of the pore dimensions is about 0.26µm for violet illumination and from 0.15µm to 1.31µm while the peak of the pore dimensions is about 0.71µm. and finally for infrared illumination the pore dimensions ranging from 0.74µm to 2.3µm while the peak of the pore dimensions is about 1.4µm.

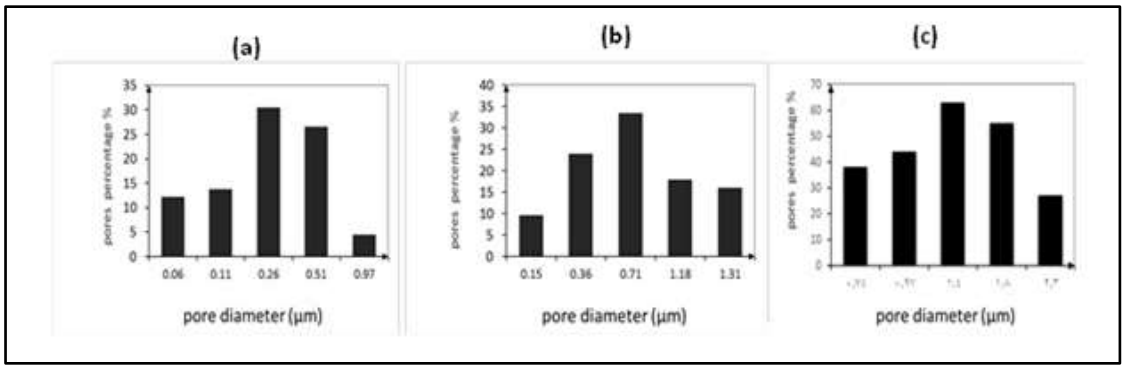

Figure 3 presents, the statistical distribution of pores with illumination wavelengths (a) 405 nm, (b) 635 nm, and (c) 810 nm.

The chemical species on mPSi structure is determined by means of FTIR absorption signals from porous silicon surface . Figures (4) shows the FTIR spectra of porous silicon substrate as a function to etching laser wavelength ; the spectra comprise the hydrogen termination bonds monohydride (Si-H) bonds, dihydride ($Si-H_2$) bonds, trihydride ($Si-H_3$), and Si-O-Si bonds. From this figure, it's clear obvious that the porous surface substrate prepared by violet illumination contains large density of hydrogen termination bonds than the substrates which prepared with red and infrared illumination. This reflects a fact that the density of ion reduction process centers which is responsible of formation the silver nanoparticles over the porous substrates is modified by laser wavelength during the etching process. The existence of Si-O-Si bonds is due the drying effects of porous silicon in ambient air, where the porous surfaces are partly oxidized as a fact to the transformation of some of hydrogen termination to oxygen termination bonds [13].

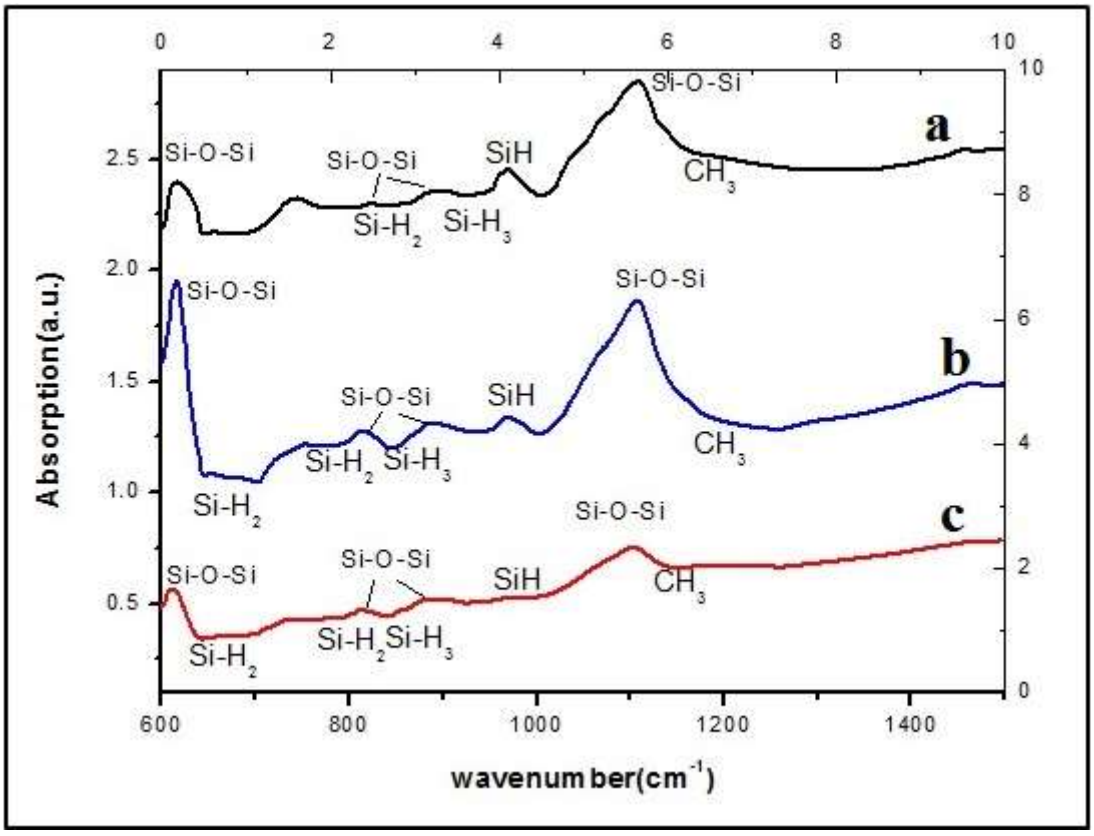

Figure 4 The effect of etching laser wavelength (a) 405 nm, (b) 635 nm, and (c) 810 nm on the FT – IR absorbance spectra of mPSi.

3.3. Structural properties of the AgNPs deposited on mPSi substrates

The morphological properties of the AgNPs layer as a function to etching laser wavelength were studied through the analysis of scanning electron microscopy image of fig. 5.

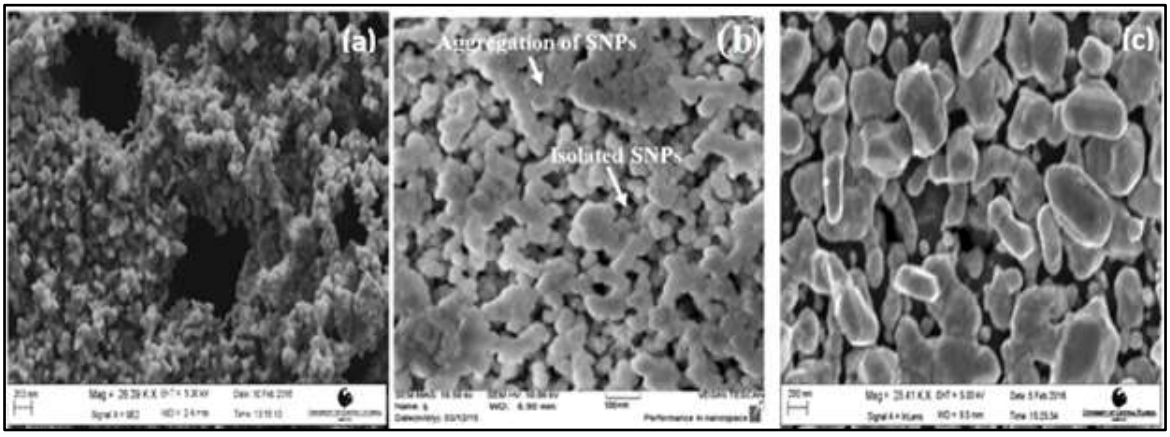

Figure 5 Display, the SEM images of AgNPs layer deposited on mPSi as a function of etching laser wavelength b) 405 nm, b) 635 nm, and c) 810 nm.

As shown from figure. 5, The morphology and the size of AgNPs were found to be a function of the mPSi properties like pore (size and shape) and the chemical species of porous surface, for violet illumination porous silicon substrate which possess the lowest pore sizes and high density of hydrogen termination, the AgNPs sizes vary from 0.61 to 3.42 nm. The maximum value of the AgNPs size is lower than the meso pore sizes so the density of the silver nano regions is likely to develop outside the pore itself. The AgNPs sizes vary from 0.61 to 3.42 µm. For red illumination porous silicon substrate, the AgNPs layer is nearly uniformly distributed over the porous layer. A closer look of figure.5b shows that only a partial coverage of the PSi surface of about 95% was got and the size of AgNPs was in the range from 200 nm to 600nm and the particle was aggregated to more than that of violet illuminated sample. The morphology and size of AgNPs on the mPSi surface of infrared illuminated sample is illustrated in figure. 5c, the size of AgNPs was in the range from 200 nm to1000 nm. The ion reduction process depends on the position and the density of the nucleation sites. And the surface of Violet illuminated porous silicon is fully coated with the Si- H bond; the number of nucleation sites for silver reduction is much greater on the other porous surface, leading to synthesize the smaller silver particles. The immersion plating of n-type PSi layer in $AgNo_3$ solution is an efficient process to synthesize AgNPs outside each pore and at the outer shell of the pore region through a redox process of silver positive ions with the Si-H bonds. These bonds represent a nucleation sites to form silver nano regions on the pore wall. This dependence of Si-H bonds (nucleation sites) on the etching wavelength is due to the fact that the etching process varies with the laser wavelength, where the absorption process of red laser wavelength would occur deeply inside the silicon wafer compared with the absorption violet wavelength which occurs at the surface of the wafer [5].

The x-ray diffraction patterns of AgNPs deposited on the PSi by immersion plating for salt concentration of 10^{-2} M for three etching laser wavelength red, and violet is presented in figure. 6.

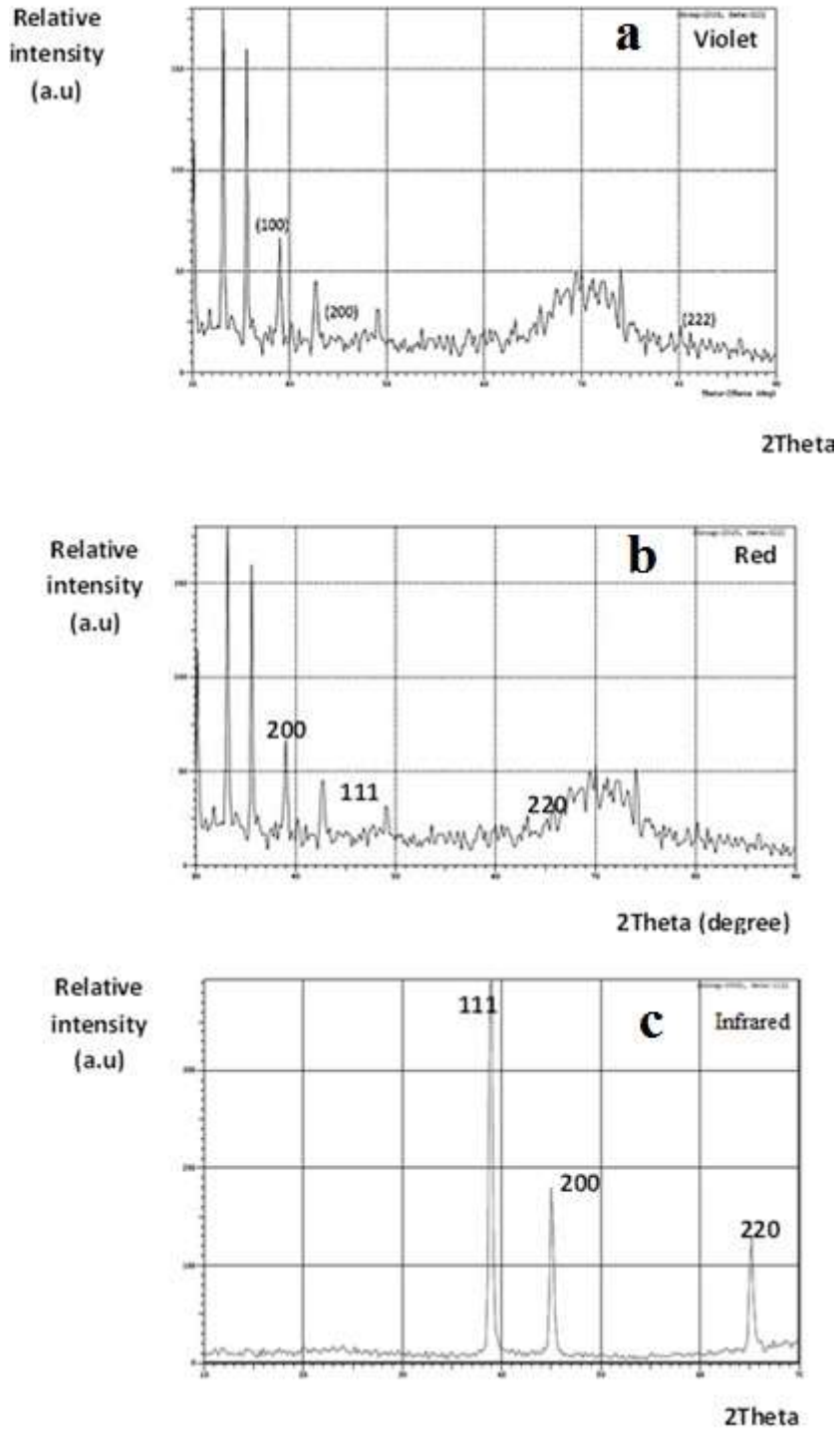

Figure 6 Shows, the XRD patterns of of AgNPs layer deposited on mPSi as a function of etching laser wavelength a) 405 nm, b) 635 nm, and c) 810 nm.

Through comparing this figure with the standard x-ray diffraction pattern of the silver, the AgNPs deposited on the mPSi surface has different peaks locations which was indexed to the reflection from (111), (200), and (220) crystal plans FCC silver correspondingly.

The experimental and standard diffraction angles of AgNPs as a function to illumination laser wavelength are obtainable in table. 2. In this Table, the modification in diffraction angle (2θ) or inter atomic space owing to the native presence of microscopic deformation (strain).

Microscopic deformation i.e., native difference of interatomic distance in AgNPs samples, is mentioned to as micro strain [4].

Table 2 Experimental and standard diffraction angles (2ɵ) of AgNPs as a function of etching laser wavelength b) 405 nm, a) 635 nm, and c) 810 nm

Laser wavelength (nm)	Experimental diffraction angle (2θ in degree)		Standard diffraction angle (2θ in degree) ASTM Standard Card
635	(111)	37.995	38.116
	(200)	44.211	44.277
	(220)	64.223	64.426
405	(111)	38.889	38.116
	(200)	45.043	44.277
	(220)	65.122	64.426
810	(111)	37.83	38.116
	(200)	44.38	44.277
	(222)	81.26	81.53

The dependence of AgNPs and its specific surface area (S) on the laser illumination wavelength reproduces new features for controlling the features of AgNPs. The width of diffraction peak is depended on the silver crystallite sizes. Large sizes leads to form sharp reflections, while a small size leads to exist a broad reflections [6] .

Table.3, demonstrations a incessant increase in the grain size of AgNPs in the plane (111) and (200) on mPSi substrate when decreasing the etching laser wavelength. The value of silver grain size as a function to etching laser wavelength 405 nm, 635 nm, and 810 nm are tabulated in table 3.

Table 3 The size of AgNPs in plane (111), (200), and (220).

Laser wavelength (nm)	Size of Silver nanoparticle in (111) plane (nm)	Size of Silver nanoparticle in (200) plane (nm)	Size of Silver nanoparticle in (220) plane (nm)	Size of Silver nanoparticle in (222) plane (nm)
635	13.4	11.87	59.57	-
405	9.28	10.4	7.09	-
810	16.2	16.21	-	30.05

The silver Nano crystallite size was measured from the peak broadening as shown in figure.7 and it can be gotten using Scherer's formula as follows [7]:

$$L = \frac{0.9\lambda}{B\cos\theta_B} \text{---------- (3)}$$

Where L is the silver Nano sizes in (nm), λ is the wavelength in (nm) of working radiation, B in (radians) is the full width at half maximum FWHM, θ_B in (radians) is the diffraction angle and (0.9) is the shape factor value.

The specific surface area (S) per mass is given as:

$$S=6000/Dp * \rho \text{---------- (4)}$$

Where S is the specific surface area, Dp is the size of the silver nanoparticle, and ρ is the density of silver 10.5 g/cm^3.[8] The highest value of specific surface area is about 80.6nm and the minimum value is about 19.3 nm for violet and red illumination respectively.

Table 4 The Specific surface area of AgNPs in plane (111), (200), and (220)

Laser wavelength (nm)	Surface area of Silver nanoparticle in (111) plane (m2 ·g−1)	Surface area of Silver nanoparticle in (200) plane (m2 ·g−1)	Surface area of Silver nanoparticle in (220) plane (m2 ·g−1)	Surface area of Silver nanoparticle in (222) plane (m2 ·g−1)
635	42.6	34.8	19.3	-
405	57.35	47.1	80.6	-
810	39.41	35.24	-	21.12

The calculated AgNPs (from SEM analysis) are greater than that calculated from XRD (Sheerer equation). This means that the SEM analysis shows the size of polycrystalline nanoparticles. In general manner, AgNPs (FCC) tend to nucleate and grow into a large group. The attendance of some bigger nanoparticles maybe documented to the tendency of AgNPs to agglomerate at high surface energy [9].

4. CONCLUSIONS

In this work; we conclude that the AgNPs were effectively prepared by laser-assisted etching process with different etching wavelength followed by a simple dipping plating process of mPSi samples. The surface morphology of mPSi was a function of laser illumination wavelength. The morphology and the sizes of the AgNPs were totally different for different laser wavelength and strongly depend on chemical species and morphology mPSi. The effect of reducing the laser wavelength will improve the density of hydrogen termination bonds and hence decreasing the AgNPs size in the prepared nano film.

REFERENCE

[1] D. Aspnes and A. Studna, "Dielectric functions and optical parameters of si, ge, gap, gaas, gasb, inp, inas, and insb from 1.5 to 6.0 ev," Physical Review B, vol. 27, p. 985, 1983.

[2] A. Ramizy, Z. Hassan, and K. Omar, "Porous silicon nanowires fabricated by electrochemical and laser-induced etching," Journal of Materials Science: Materials in Electronics, vol. 22, pp. 717-723, 2011.

[3] F. A. Harraz, A. A. Ismail, H. Bouzid, S. Al-Sayari, A. Al-Hajry, and M. Al-Assiri, "Surface-enhanced Raman scattering (SERS)-active substrates from silver plated-porous silicon for detection of crystal violet," Applied Surface Science, vol. 331, pp. 241-247, 2015.

[4] A. M. Zohbi, "DESIGN AND FABRICATION OF OPTICAL FILTERS FOR LONG WAVELENGTH SPECTROSCOPY APPLICATION," The University of North Carolina at Charlotte, 2012.

[5] Y. Lai, J. Wang, T. He, and S. Sun, "Improved Surface Enhanced Raman Scattering for Nanostructured Silver on Porous Silicon for Ultrasensitive Determination of 2, 4, 6-Trinitrotoluene," Analytical Letters, vol. 47, pp. 833-842, 2014.

[6] J. Langford, D. Louër, and P. Scardi, "Effect of a crystallite size distribution on X-ray diffraction line profiles and whole-powder-pattern fitting," Journal of applied crystallography, vol. 33, pp. 964-974, 2000.

[7] A. Monshi, M. R. Foroughi, and M. R. Monshi, "Modified Scherrer equation to estimate more accurately nano-crystallite size using XRD," World Journal of Nano Science and Engineering, vol. 2, p. 154, 2012.

[8] Y. Sun and Y. Xia, "Shape-controlled synthesis of gold and silver nanoparticles," Science, vol. 298, pp. 2176-2179, 2002.

[9] T. Theivasanthi and M. Alagar, "Electrolytic synthesis and characterizations of silver nanopowder," arXiv preprint arXiv:1111.0260, 2011.

[10] Theivasanthi, T., and M. Alagar. "Nano sized copper particles by electrolytic synthesis and characterizations." International Journal of Physical Sciences 6.15 (2011): 3662-3671.

[11] J.Hayder Adawyia, M.Alwan Alwan, A.Jabbar Allaa"Optimizing of porous silicon morphology for synthesis of silver Nanoparticles"Microporous and Mesoporous Materials 227 (2016) 152e160.

[12] J. DeBoer, S. Lewis, P.J. Hesketh, J.L. Gole, Method for signal extraction from chemical sensor response, Invention disclosure Georgia Institute of Technology, February, 2004.

[13] N. Naderi, M.R. Hashim , T.S.T. Amran" Enhanced physical properties of porous silicon for improved hydrogen gas sensing" Superlattices and Microstructures 51 (2012) 626–634